

Understanding deep learning via decision boundary

Shiye Lei* Fengxiang He[†] Yancheng Yuan[‡] Dacheng Tao[†]

Abstract

This paper discovers that the neural network with lower decision boundary (DB) variability has better generalizability. Two new notions, *algorithm DB variability* and (ϵ, η) -*data DB variability*, are proposed to measure the decision boundary variability from the algorithm and data perspectives. Extensive experiments show significant negative correlations between the decision boundary variability and the generalizability. From the theoretical view, two lower bounds based on algorithm DB variability are proposed and do not explicitly depend on the sample size. We also prove an upper bound of order $\mathcal{O}\left(\frac{1}{\sqrt{m}} + \epsilon + \eta \log \frac{1}{\eta}\right)$ based on data DB variability. The bound is convenient to estimate without the requirement of labels, and does not explicitly depend on the network size which is usually prohibitively large in deep learning.

1 Introduction

Neural networks (NNs) have achieved significant success in vast applications [31, 58], including computer vision [20], natural language processing [5], and data mining [59]. However, the advance of NNs is arduous to be characterized by conventional statistical learning theory based on hypothesis complexity [41], such as VC-dimension [57] and Rademacher complexity [2]. According to the conventional theory, models of larger hypothesis complexity possess worse generalizability, while neural networks are usually over-parameterized but have excellent generalizability.

In this paper, we attempt to explain the excellent generalizability of deep learning from the perspective of decision boundary (DB) variability. Intuitively, the decision boundary variability of a neural networks is largely determined by two means: (1) the randomness introduced by the optimization algorithm, and (2) the fluctuations of the training data when they are sampled from the data generating distribution. Following this intuition, we design two terms, *algorithm DB variability* and (ϵ, η) -*data DB variability*, to measure the DB variability.

Algorithm DB variability measures the variability of DBs in different training repeats. We conduct extensive experiments on the CIFAR-10/100 datasets [30] to explore which factors would determine algorithm DB variability. We visualize the trend of the algorithm DB variability with respect to (*w.r.t.*) training strategies, training time, sample sizes, and label noise ratios. The empirical results demonstrate that algorithm DB variability has (1) negative correlations with the training time and the sample size, (2) a positive correlation with the label noise, and (3) a negative correlation with the generalizability (or, test accuracy, in experiments). From the theoretical

*S. Lei is associated with School of Computer Science, Faculty of Engineering, the University of Sydney, Darlington NSW 2008, Australia. This work was completed when he was an intern at JD Explore Academy. Email: slei5230@uni.sydney.edu.au.

[†]F. He and D. Tao are associated with JD Explore Academy, JD.com Inc., BDA Beijing 100176, China. Email: fengxiang.f.he@gmail.com and dacheng.tao@gmail.com.

[‡]Y. Yuan is associated with Department of Applied Mathematics, The Hong Kong Polytechnic University. Email: yancheng.yuan@polyu.edu.hk.

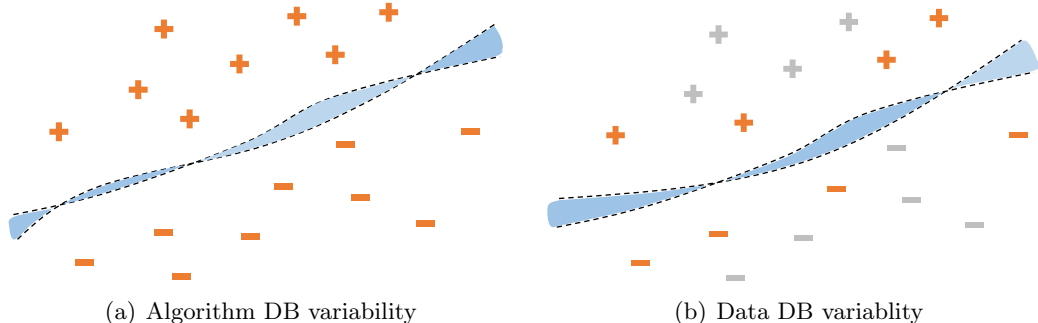


Figure 1: An illustration of decision boundary variability. (a) Two dashed curves denote the decision boundaries of the model trained on the orange points with different repeats, respectively, and the blue mismatch region is connected to the algorithm DB variability; (b) Two dashed curves denote the decision boundaries of the model trained on the orange points and all (orange and gray) points, respectively, and the blue mismatch region is connected to the data DB variability.

view, we prove two lower bounds based on the algorithm DB variability, which fully support our experiments.

(ϵ, η) -**data DB variability** is proposed to characterize the decision boundary from the view of the randomness in training data. Given a neural network, if its decision boundary can be “reconstructed” by training a network with the same architecture from the scratch on a smaller η -subset (which contain $\eta\%$ examples of the source training set), while the “error” of the reconstruction is not larger than ϵ , we call the model has (ϵ, η) -data DB variability. Specifically, we may define the reconstruction error as the approximation error of the reconstructed decision boundary on the whole training set. Moreover, an η - ϵ curve can be drawn numerically. The area under the η - ϵ curve could be an informative indicator for characterizing the generalization of NNs. An $\mathcal{O}\left(\frac{1}{\sqrt{m}} + \epsilon + \eta \log \frac{1}{\eta}\right)$ generalization bound based on the (ϵ, η) -data DB variability is proved, which demonstrates the relationship between the generalization of NNs and DB variability. In contrast to many existing generalization bounds based on hypothesis complexity that require the access to the weight norm, our bounds only need the predictions. This brings significant advantages in empirically approximating the generalization bound in (1) black-model settings, where model parameters are unavailable, and (2) over-parameterized settings, where calculating the weight norm is of a prohibitively high computing burden.

To our best knowledge, this is the first work on explaining deep learning via the variability of decision boundary. Our research also sheds light to understanding a variety of interesting phenomena, including the entropy and the complexity of decision boundary. Through the lens of decision boundary variability, we may also design novel algorithms via reducing the decision boundary variability.

2 Related works

Deep learning theory. In learning theory, generalizability refers to the capability of well-trained models predicting on unseen data. Conventional theory suggests that the generalizability has a negative correlation with the hypothesis complexity [41], such as VC-dimension [57] and Rademacher complexity [2]: models with larger complexity fit the training data better. This is usually summarised as the “bias-variance trade-off”. This principle faces significant challenges in deep learning [16, 37].

Zhang et al. [63] demonstrate that neural networks can near-perfectly fit noisy labels (which suggests that deep learning has an extremely large Rademacher complexity), but still have impressive generalization performance. This conflict draws attentions of numerous researchers [3, 22, 42]. Belkin et al. [3] show the unusual double descent phenomena of the training error *w.r.t.* model size following by works [32, 42], which further sheds shadows to the “variance-bias trade-off”.

Many works attribute the success of neural networks to the effectiveness of the stochastic gradient descent (SGD) algorithm [4, 15, 17, 56]. For example, Jin et al. [25] show that SGD can escape from the local minima. The loss landscape of the networks has also been extensively analysed and it has been proven that there is no spurious local minima for linear NNs [29, 34, 67]. Nevertheless, this elegant property does not hold for general networks where non-linear activation functions are involved [12, 18]. Recent study also attempts to explore the implicit bias of neural networks in the over-parameterized regime. Soudry et al. [53] show that the over-parameterized networks converge to the max-margin solution when the training data is linear-separable. Some other research has also been conducted along this line [8, 23, 36].

Empirical studies have also attempted to explain the decent performance of networks by uncovering their learning properties [24, 43, 46]. For instance, neural networks are shown tend to fit the low-frequency information first [47, 61] and then gradually learn fit more complex patterns [26] during the training procedure. He and Su [19] show that neural networks own the unique property of local elasticity that the predictions on the input data \mathbf{x}' will not be significantly perturbed, when the neural net is updated via SGD at the training example \mathbf{x} if \mathbf{x}' is “dissimilar” to \mathbf{x} . Similar phenomena are also observed by Fort et al. [11]. Besides, Pappayan et al. [45] uncover a novel phenomenon, neural collapse, which sheds light on interpreting the effectiveness of deep models [10].

Decision boundaries in neural networks. Decision boundary, which partitions the input space with different labels, is an important notion in machine learning. Recent studies attempt to understand neural networks from the aspect of decision boundaries [21, 27, 28]. Alfarra et al. [1] employ the tropical geometry to represent the decision boundary of neural networks. Guan and Loew [14] empirically show a negative correlation between the complexity of decision boundary and the generalization performance of neural networks. Mickisch et al. [40] reveal an insightful phenomenon that the distance from data to the decision boundary continuously decreases during the training. More recently, researchers uncover that neural networks only rely on the most discriminative or the simplest features to construct the decision boundary [44, 49]. Besides, Samangouei et al. [48] also explain the predictions of neural networks via constructing examples crossing the decision boundary. To our best knowledge, this paper is the first work on (1) theoretically characterizing the complexity of decision boundary via the new measure, decision boundary variability, and (2) explaining the negative correlation between the generalizability and decision boundary variability.

Adversarial training. It has been shown that the adversarial examples, which are created by adding non-perceivable perturbation on data, can completely mislead the predictions of neural networks [7, 13, 33, 55]. To tackle this problem, adversarial training is proposed to improve the robustness of the neural networks through training on adversarial examples [6, 38]. Nevertheless, Su et al. [54] show a trade-off between the robustness and the generalization performance of neural networks. Zhang et al. [64] explain the trade-off as follows: adversarial training leads to the underfitting on the “normal” samples and thus undermines the model accuracy. Further, they mitigate this trade-off between robustness and accuracy by disentangling the robust error into a natural error and a boundary error, and then design new algorithms to decrease the boundary error. Moreover, Zhang et al. [65] alleviate the trade-off by assigning small weights to “non-important” samples for reducing the model capacity and develop a reweighting framework to improve the robustness while preserving the accuracy.

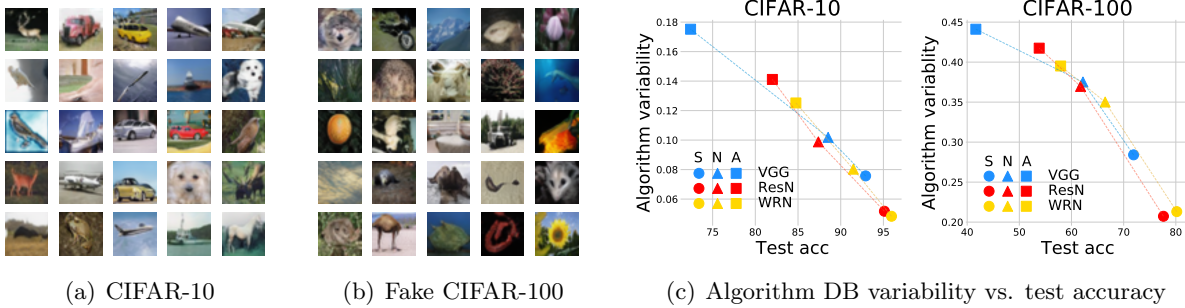


Figure 2: Algorithm decision boundary variability on CIFAR-10 and CIFAR-100. (a) Examples of fake CIFAR-10 images generated by conditional BigGAN. (b) Examples of fake CIFAR-100 images generated by conditional BigGAN. (c) Scatter plots of algorithm DB variability to accuracy on test set with different architectures and training strategies on CIFAR-10 and CIFAR-100. The colors of blue, red, and yellow points denote the architectures of VGG-16 (VGG), ResNet-18 (ResN), and WideResNet-28 (WRN), respectively. The shapes of \bullet , \blacktriangle , and \blacksquare designate the training strategies of standard training (S), non-data-augmentation training (N), and adversarial training (A), respectively. Each point is calculated and then averaged on 10 trials.

3 Preliminaries

We denote the training set by $\mathcal{S} = \{(\mathbf{x}_i, y_i), i = 1, \dots, m\}$, where $\mathbf{x}_i \in \mathbb{R}^n$, n is the dimension of input data, $y_i \in [k] = \{1, \dots, k\}$, k is the number of classes, and $m = |\mathcal{S}|$ is the training sample size. We assume that (\mathbf{x}_i, y_i) are independent and identically distributed (i.i.d.) random variables drawn from the data generating distribution \mathcal{D} . Denote the classifier as $f_{\theta}(\mathbf{x}) : \mathbb{R}^n \rightarrow \mathbb{R}^k$, which is a neural network parameterized by θ . The output of $f_{\theta}(\mathbf{x})$ is a k -dimensional vector and is assumed to be a discrete probability density function. Let $f_{\theta}^{(i)}(\mathbf{x})$ be the i -th component of $f_{\theta}(\mathbf{x})$, hence $\sum_{i=1}^k f_{\theta}^{(i)}(\mathbf{x}) = 1$. We define $T(f_{\theta}, \mathbf{x}) = \{i \in \{1, \dots, k\} | f_{\theta}^{(i)}(\mathbf{x}) = \max_j f_{\theta}^{(j)}(\mathbf{x})\}$ to denote the set of predicted labels by f_{θ} on \mathbf{x} . Due to the randomness of the learning algorithm \mathcal{A} , let $\mathbb{Q}(\theta) = \mathcal{A}(\mathcal{S})$ denote the posteriori distribution returned by the learning algorithm \mathcal{A} leveraged on the training set \mathcal{S} . Hence, we focus on the *Gibbs classifier* (a.k.a. random classifier) $f_{\mathbb{Q}} = \{f_{\theta} | \theta \sim \mathbb{Q}\}$. 0-1 loss is employed in this paper, and the expected risks in terms of θ and \mathbb{Q} are defined as:

$$\mathcal{R}_{\mathcal{D}}(\theta) = \mathbb{E}_{(\mathbf{x}, y) \sim \mathcal{D}} [\mathbb{I}(y \notin T(f_{\theta}, \mathbf{x}))]$$

and

$$\mathcal{R}_{\mathcal{D}}(\mathbb{Q}) = \mathbb{E}_{(\mathbf{x}, y) \sim \mathcal{D}} \mathbb{E}_{\theta \sim \mathbb{Q}} [\mathbb{I}(y \notin T(f_{\theta}, \mathbf{x}))],$$

respectively. Here $\mathbb{I}(\cdot)$ is the indicator function. Since the data generating distribution \mathcal{D} is unknown, evaluating the expected risk $\mathcal{R}_{\mathcal{D}}$ is not practical. Therefore, it is a practical way to estimate the expected risk by the empirical risk $\mathcal{R}_{\mathcal{S}}$, which is defined as:

$$\mathcal{R}_{\mathcal{S}}(\theta) = \mathbb{E}_{(\mathbf{x}, y) \sim \mathcal{S}} [\mathbb{I}(y \notin T(f_{\theta}, \mathbf{x}))] = \frac{1}{m} \sum_{i=1}^m \mathbb{I}(y_i \notin T(f_{\theta}, \mathbf{x}_i))$$

$$\mathcal{R}_{\mathcal{S}}(\mathbb{Q}) = \mathbb{E}_{(\mathbf{x}, y) \sim \mathcal{S}} \mathbb{E}_{\theta \sim \mathbb{Q}} [\mathbb{I}(y \notin T(f_{\theta}, \mathbf{x}))] = \frac{1}{m} \sum_{i=1}^m \mathbb{E}_{\theta \sim \mathbb{Q}} [\mathbb{I}(y_i \notin T(f_{\theta}, \mathbf{x}_i))],$$

where $(\mathbf{x}_i, y_i) \in \mathcal{S}$ and $m = |\mathcal{S}|$.

3.1 Decision boundary

Intuitively, if the output k -dimensional vector $f_{\theta}(\mathbf{x})$ on the input example \mathbf{x} has a tie, *i.e.*, more than one entries of the vector have the maximum value, then \mathbf{x} is considered to locate on the decision boundary of f_{θ} . Formally, the decision boundary can be formally defined as below.

Definition 3.1 (decision boundary). Let $f_{\theta}(\mathbf{x}) : \mathbb{R}^n \rightarrow \mathbb{R}^k$ be a neural network for classification parameterized by θ , where n and k are the dimensions of input and output, respectively. Then, the *decision boundary* of f_{θ} is defined by

$$\{\mathbf{x} \in \mathbb{R}^n | \exists i \neq j \in [k], f_{\theta}^{(i)}(\mathbf{x}) = f_{\theta}^{(j)}(\mathbf{x}) = \max_q f_{\theta}^{(q)}(\mathbf{x})\}.$$

Consequently, we have the following remark.

Remark 3.2. (1) If an input example (\mathbf{x}, y) is not located on the decision boundary of f_{θ} , $T(f_{\theta}, \mathbf{x})$ is a singleton, and we have,

$$\mathbb{I}(y \notin T(f_{\theta}, \mathbf{x})) = \mathbb{I}(y \neq T(f_{\theta}, \mathbf{x})).$$

(2) If the input \mathbf{x} is a boundary point, in practice, we randomly draw a label from the set $T(f_{\theta}, \mathbf{x})$ as the prediction of f_{θ} on \mathbf{x} .

3.2 Adversarial training

Adversarial training (AT) can enhance the adversarial robustness of neural networks against adversarial examples, which is generated through a popular approach projected gradient descent (PGD) [39] in our empirical studies as an example. More specifically, adversarial training can be formulated as solving the minimax-loss problem as follows,

$$\min_{\theta} \frac{1}{m} \sum_{i=1}^m \max_{\|\mathbf{x}'_i - \mathbf{x}_i\| \leq \gamma} \ell(f_{\theta}(\mathbf{x}'_i), y_i),$$

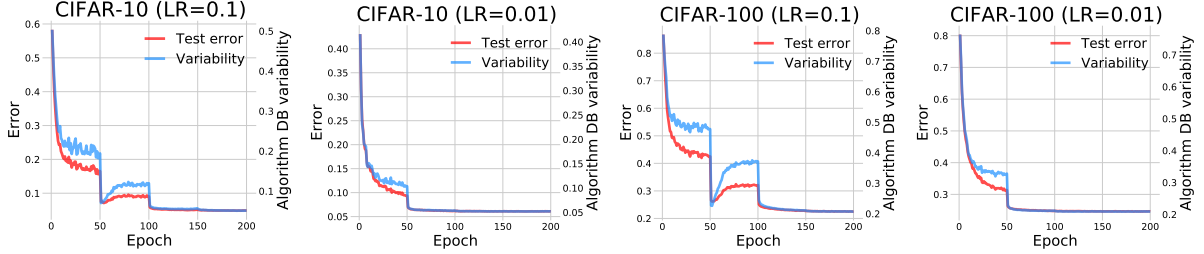
where γ is the *radius* to limit the distance between adversarial examples and original examples. Intuitively, adversarial training enlarges the distances from training examples to decision boundaries to at least γ , which is formerly very closed to the decision boundary.

3.3 Shapley value

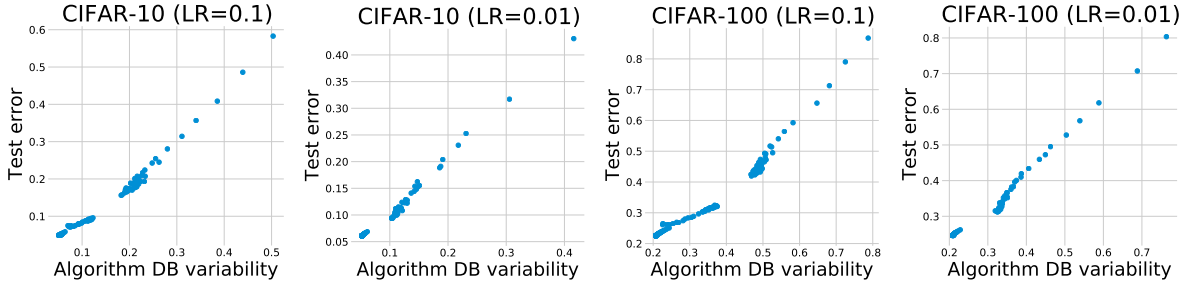
In cooperative game theory, Shapley value is a tool to analyze the surplus brought by each player [51]. Similarly, if we treat the notion of “player” as feature contained in the dataset, Shapley value can be used to measure the contributions of features to the predictions outputted by neural networks [35]. For each input \mathbf{x} , we assume that \mathbf{x} consists of p features, *i.e.*, $\mathbf{x} = \{F_1, \dots, F_p\}$. Then, the Shapley value of feature F_j *w.r.t.* the model f_{θ} is as follows,

$$\phi_j(f_{\theta}) = \sum_{S \subseteq \{F_1, \dots, F_p\} \setminus \{F_j\}} \frac{|S|!(p - |S| - 1)!}{p!} \mathbb{E}_{\mathbf{x} \sim S} [\mathbb{I}(T(f_{\theta}, \mathbf{x} \cup \{F_j\}) \neq T(f_{\theta}, \mathbf{x}))].$$

According to the above definition of Shapley value, a small Shapley value ϕ_j indicates that feature F_j only has little impact on the prediction of the network f_{θ} . Therefore, the set of Shapley values $\{\phi_1, \dots, \phi_p\}$ partly reveal how the well-trained network extracts knowledge from the input data and produces the predictions.



(a) Algorithm DB variability and test error vs. training time



(b) Test error vs. algorithm DB variability

Figure 3: (a) Plots of algorithm DB variability and test error as functions of training time (LR is learning rate). (b) Scatter plots of test error to algorithm DB variability (LR is learning rate). The points are collected from different epochs. Each curve and point is calculated and then averaged on 10 trials.

4 Algorithm decision boundary variability

Due to the randomness of learning algorithms, there is no doubt that the parameters have a substantial variation in training repeats. However, *do the decision boundaries in the different training repeats have a large discrepancy?* Quantitatively, we define the algorithm decision boundary variability (AV) to measure the variability of DBs caused by the randomness of algorithms in different training repeats.

Definition 4.1 (algorithm decision boundary variability). Let $f_{\theta}(\mathbf{x}) : \mathbb{R}^n \rightarrow \mathbb{R}^k$ be a neural network for classification parameterized by θ . Suppose $\mathbb{Q}(\theta)$ is the distribution over θ . Then, the algorithm decision boundary variability for $f_{\mathbb{Q}}$ on \mathcal{D} is defined as below,

$$AV(f_{\mathbb{Q}}, \mathcal{D}) = \mathbb{E}_{(\mathbf{x}, y) \sim \mathcal{D}} \mathbb{E}_{\theta, \theta' \sim \mathbb{Q}} [\mathbb{I}(T(f_{\theta}, \mathbf{x}) \neq T(f_{\theta'}, \mathbf{x}))],$$

where $T(f_{\theta}, \mathbf{x}) = \{i \in [k] | f_{\theta}^{(i)}(\mathbf{x}) = \max_j f_{\theta}^{(j)}(\mathbf{x})\}$.

According to the definition, algorithm DB variability reflects the similarity of decision boundaries during different training repeats. An illustration of algorithm DB variability is provided in Figure 1(a).

4.1 Algorithm DB variability and generalization

To explore the relationship between the algorithm DB variability and generalization in neural networks, we conduct experiments with various popular network architectures, VGG-16 [52], ResNet-18 [20], and WideResNet-28 [62], on standard datasets, CIFAR-10 and CIFAR-100. In detail, VGG-16

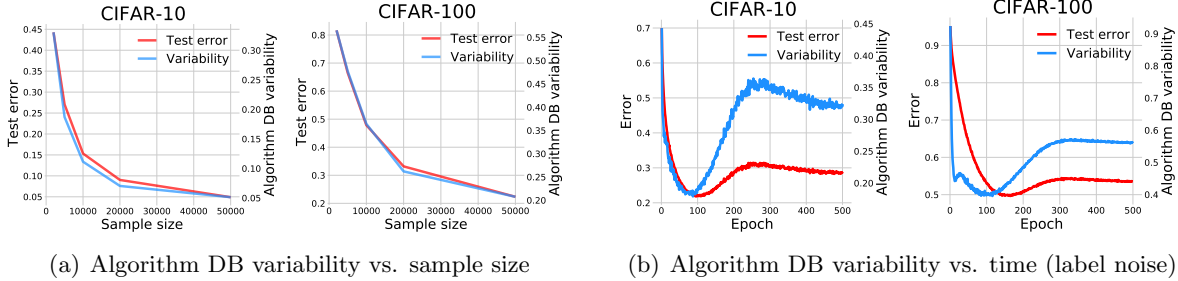


Figure 4: (a) Plots of algorithm DB variability and test error as functions of training sample size on CIFAR-10 and CIFAR-100. (b) Plots of algorithm DB variability and test error as functions of training time with the existence of 20% label noise on CIFAR-10 and CIFAR-100. Each curve is calculated and then averaged on 10 trials.

[52], ResNet-18 [20], and WideResNet-28 [62] are optimized by standard, non-data-augmentation and adversarial training, respectively, until the training procedure converges. Each training setting (determined by different datasets, architectures, and/or training strategies) is repeated for 10 trials with different random seeds to estimate the parameter distribution $\mathbb{Q}(\theta)$. In order to simulate the data generating distribution, we trained two conditional BigGANs [66] to produce 100,000 fake (or, synthetic) images for CIFAR-10 and CIFAR-100, respectively. Examples of fake images are shown in Figure 2(a) and 2(b).

These generative fake images enables estimating the algorithm DB variability. In every training setting, we plot the average test accuracy vs. the algorithm DB variability; as shown in Figure 2(c). From the plots, we obtain the following four observations: (1) adversarial training dramatically decreases the test accuracy and promotes the algorithm DB variability compared to the standard training. (2) data augmentation decreases the algorithm decision boundary variability. Intuitively, the images augmented by cropping or flipping are still located on the data generating distribution, so data augmentation can expand the training set. Hence, the expanded training set can characterize wider decision boundaries on the data generating distribution; (3) WideResNet has better test accuracy and lower algorithm DB variability than ResNet and VGG; and (4) a negative correlation exists between the test accuracy and the algorithm DB variability. Based on these observations, we propose the following conjecture.

Hypothesis 4.2. *Neural networks with smaller algorithm decision boundary variability on the data generating distributions possess better generalization performance.*

We then conduct experiments on the algorithm DB variability *w.r.t.* training time, sample size, and label noise to concrete this hypothesis to verify our hypothesis.

4.2 Algorithm DB variability and training time

To investigate the relationship between algorithm DB variability and training time, we train 40 ResNet-18 with different initial learning rates of 0.1 and 0.01 on CIFAR-10 and CIFAR-100. Then, the algorithm DB variability and test error are calculated at each epoch; see Figure 3(a). From the plots, two observations can be obtained: (1) algorithm DB variability and test error share a very similar curve *w.r.t.* the training time; and (2) algorithm DB variability decreases during the training process. The decline of algorithm DB variability shows that the interpolation on examples reduces the variability of decision boundaries on data generating distribution. As shown in Figure 3(b), we

collect the points of (algorithm DB variability, test error) from different epochs, and the scatter plots present a significant positive correlation between test error and the algorithm DB variability, and thus supports Hypothesis 4.2.

4.3 Algorithm DB variability and sample size

We next investigate how sample size influences the algorithm DB variability. 100 ResNet-18 are trained on five training sample sets of different sizes randomly drawn from CIFAR-10 and CIFAR-100, while all irrelevant variables are strictly controlled. Then, the algorithm DB variability and test error are calculated in all cases; see Figure 4(a). From the plots, we have the following two observations: (1) test error and algorithm DB variability share a very similar curve *w.r.t.* the training sample size; (2) larger sample size, which intuitively helps obtain a more smooth estimation of the decision boundary, also contributes to smaller algorithm DB variability; and (3) there is a significant positive correlation between test error and algorithm DB variability, which fully supports our argument of Hypothesis 4.2.

4.4 Algorithm DB variability and label noise

Belkin et al. [3], Nakkiran et al. [42] show a surprising epoch-wise double descent of test error, especially with the existence of label noise. We explore in this section the trend of algorithm DB variability when the label noise exists. 20 ResNet-10 are trained for 500 epochs with a constant learning rate of 0.0001 on CIFAR-10 and CIFAR-100 with 20% label noise. We clarify that the noise labels remain constant in different training repeats, which is necessary to estimate the algorithm DB variability. Then, the average test error and algorithm DB variability are calculated at every training epoch, as shown in Figure 4(b). From the plots, two observations can be derived: (1) the algorithm DB variability also undergoes an epoch-wise double descent during the training process, especially in the left panel of Figure 4(b); and (2) test error and algorithm DB variability still share a very similar curve *w.r.t.* the training time with the existence of label noise, which implies that factors influence the generalization of networks can also have an influence on the algorithm DB variability. Hence, algorithm DB variability is an excellent indicator for the generalization ability of networks.

Here, we propose an insightful explanation about the epoch-wise double descent phenomenon of the data DB variability *w.r.t.* the training time: the increase of algorithm DB variability shows that fitting the noisy examples has a considerable effect on the formation of decision boundaries on data generating distribution. However, the algorithm DB variability decreases when the training proceeds further. This indicates that the negative effects brought from fitting the noisy training examples is gradually weakened. In other words, as the training proceeds, neural networks can automatically reduce the impact brought from interpolating hard-to-fit examples, which is insightful in explaining the decent generalizability of neural networks.

4.5 DB variability and feature extraction stability

Apparently, neural networks also rely on the features of the input data to make the predictions. Based on the Shapley value, we may evaluate the impacts of single features in making predictions. If the proportion of each features employed by the well-trained network is less fluctuated during the repeated training, the neural network is called to possess a strong feature extraction stability. In this section, we explore the relationship between the algorithm DB variability and the feature extraction stability.

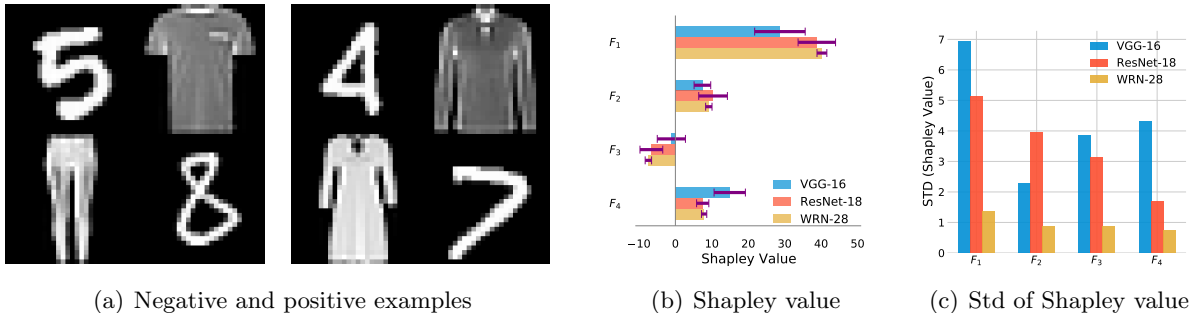


Figure 5: (a) Examples of synthetic binary dataset; (b) Shapley values on the synthetic dataset; (c) Standard deviation (std) of Shapley values on the synthetic dataset.

We first construct a binary classification dataset with four notable features based on the MNIST and Fashion-MNIST [60] datasets, as shown in Figure 5(a), where the top left part of the image shows MNIST digits from class $\{5, 4\}$, the top right part is from the classes $\{\text{T-shirt, pullover}\}$ of Fashion-MNIST, the bottom left part is from the classes $\{\text{trouser, dress}\}$ of Fashion-MNIST, and the bottom right part shows MNIST digits from class $\{8, 7\}$. We train VGG-16, ResNet-18, and WideResNet-28 on the synthetic binary classification dataset repeatedly for 10 times with different random seeds, respectively, and then compute their Shapley values for each well-trained model.

The results are presented in Figure 5(b) and 5(c). Figure 5(b) shows the Shapley values of different features (F_1, F_2, F_3, F_4) *w.r.t.* different models, where the error bars, *i.e.*, the standard deviations, are represented by the purple lines. The error bar reflects the network’s stability of extracting feature from the dataset. The standard deviation of Shapley value is presented separately in Figure 5(c). From the figure, we may obtain an observation that WideResNet-28, which possesses better the generalization performance, also owns much smaller standard deviation of Shapley value, than VGG-16 and ResNet-18. Therefore, given the positive correlation between the generalization performance, algorithm DB variability, and feature extraction stability, we reasonably conjecture that the algorithm DB variability reflect the feature extraction stability and thus is closely connected to the network’s generalizability.

4.6 Theoretical Evidence

In this section, we explore and develop the theoretical foundations for the algorithm decision boundary variability on data generating distributions.

In most practical cases, the dimension of decision boundaries is smaller than the data space. For example, the decision boundary in a three-dimensional data space is usually two. Thus, we may make the following mild assumption.

Assumption 4.3. The decision boundary of the classifier network f_{θ} on data generating distribution \mathcal{D} is a set with measure zero.

We then have the following lemma.

Lemma 4.4. Let $f_{\theta}(\mathbf{x}) : \mathbb{R}^n \rightarrow \mathbb{R}^k$ be a classifier network parameterized by θ . If Assumption 4.3 holds for all $\theta \sim \mathbb{Q}$, then, for all $i \in \{1, \dots, k\}$, we have

$$\mathbb{E}_{(\mathbf{x}, y) \sim \mathcal{D}} [\mathbb{I}(i \in T(f_{\theta}, \mathbf{x}))] = \mathbb{E}_{(\mathbf{x}, y) \sim \mathcal{D}} [\mathbb{I}(T(f_{\theta}, \mathbf{x}) = i)]$$

and

$$\mathbb{E}_{(\mathbf{x}, y) \sim \mathcal{D}} [\mathbb{I}(i \notin T(f_{\theta}, \mathbf{x}))] = \mathbb{E}_{(\mathbf{x}, y) \sim \mathcal{D}} [\mathbb{I}(T(f_{\theta}, \mathbf{x}) \neq i)].$$

Then, can we prove the following theorem.

Theorem 4.5 (lower bound on expected risk). *Let $f_{\boldsymbol{\theta}}(\mathbf{x}) : \mathbb{R}^n \rightarrow \mathbb{R}^k$ be a neural network for classification parameterized by $\boldsymbol{\theta}$. Suppose $\mathbb{Q}(\boldsymbol{\theta})$ is the distribution over $\boldsymbol{\theta}$. Then, if Assumption 4.3 holds for all $\boldsymbol{\theta} \sim \mathbb{Q}$, we have,*

$$\mathcal{R}_{\mathcal{D}}(\mathbb{Q}) \geq \frac{AV(f_{\mathbb{Q}}, \mathcal{D})}{2},$$

where $AV(f_{\mathbb{Q}}, \mathcal{D})$ is the algorithm DB variability for $f_{\mathbb{Q}}$ on data generating distribution \mathcal{D} .

Theorem 4.5 provides a lower bound on the expected risk $\mathcal{R}_{\mathcal{D}}(\mathbb{Q})$ based on the algorithm DB variability $AV(f_{\mathbb{Q}}, \mathcal{D})$. Moreover, when we consider the binary classification, *i.e.*, $k = 2$, there is a tighter lower bound.

Theorem 4.6 (lower bound for binary case). *Let $f_{\boldsymbol{\theta}}(\mathbf{x}) : \mathbb{R}^n \rightarrow \mathbb{R}^2$ be a binary classifier network parameterized by $\boldsymbol{\theta}$ and let $\mathbb{Q}(\boldsymbol{\theta})$ be the distribution over $\boldsymbol{\theta}$. Suppose the expected risk $\mathcal{R}_{\mathcal{D}}(\mathbb{Q}) \leq \frac{1}{2}$ and Assumption 4.3 hold for all $\boldsymbol{\theta} \sim \mathbb{Q}$, then we have*

$$\mathcal{R}_{\mathcal{D}}(\mathbb{Q}) \geq \frac{1 - \sqrt{1 - 2AV(f_{\mathbb{Q}}, \mathcal{D})}}{2}.$$

These lower bounds present that the Gibbs classifier $f_{\mathbb{Q}}$ possesses a significant expected risk when its algorithm DB variability is large. As such, a small algorithm DB variability decreases the bound and facilitates generalization performance of $f_{\mathbb{Q}}$.

5 Data decision boundary variability

In the previous sections, we introduced the algorithm DB variability, which measures the decision boundary variability caused by the randomness of learning algorithms. In this section, we define the data DB variability to characterize decision boundary variability caused by the randomness in training data.

Definition 5.1 (data decision boundary variability). Let $f_{\boldsymbol{\theta}}(\mathbf{x}) : \mathbb{R}^n \rightarrow \mathbb{R}^k$ be a neural network for classification parameterized by $\boldsymbol{\theta}$, where $\boldsymbol{\theta} \sim \mathcal{A}(\mathcal{S})$ is returned by leveraging the stochastic learning algorithm \mathcal{A} on the training set \mathcal{S} , which is sampled from the data generating distribution \mathcal{D} . We term $\mathcal{S}_{\eta} \subset \mathcal{S}$ as a η -subset of \mathcal{S} if $\frac{|\mathcal{S}_{\eta}|}{|\mathcal{S}|} = \eta$. Then, if we fixed η and

$$\inf_{\mathcal{S}_{\eta} \subset \mathcal{S}} \mathbb{E}_{\mathcal{D}} \mathbb{E}_{\boldsymbol{\theta} \sim \mathcal{A}(\mathcal{S}), \boldsymbol{\theta}' \sim \mathcal{A}(\mathcal{S}_{\eta})} [\mathbb{I}(T(f_{\boldsymbol{\theta}}, \mathbf{x}) \neq T(f_{\boldsymbol{\theta}'}, \mathbf{x}))] = \epsilon,$$

the decision boundary of $f_{\mathcal{A}(\mathcal{S})}$ is said to possess a (ϵ, η) -data decision boundary variability.

An illustration of data DB variability is presented in Figure 1(b). The data decision boundary variability contains two parameters of ϵ and η , respectively. That Gibbs classifier $f_{\mathcal{A}(\mathcal{S})}$ has a (ϵ, η) -data DB variability means that only the proportion of η of \mathcal{S} , *i.e.*, \mathcal{S}_{η} (which can be considered as “support vector set”) is enough to reconstruct a similar decision boundary with the reconstruction error ϵ . The data DB variability can also be connected with the complexity of decision boundaries if we assume that simpler decision boundaries rely on a smaller number of “support vectors”; we provide a detailed discussion in Section 6.2.

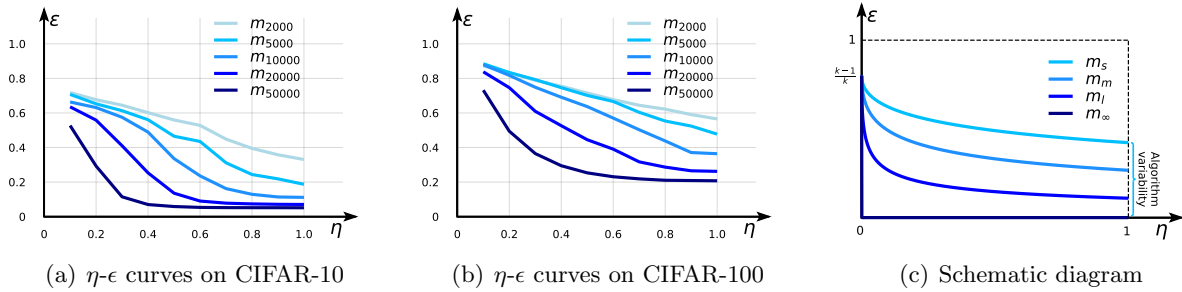


Figure 6: (a) The η - ϵ curves on CIFAR-10 with different training sample sizes 2000 (m_{2000}), 2000 (m_{2000}), 10000 (m_{10000}), 20000 (m_{20000}), and 50000 (m_{50000}), respectively. (b) The η - ϵ curves on CIFAR-100 with different training sample sizes. (c) The schematic diagram of the η - ϵ curves *w.r.t.* small (m_s), medium (m_m), large (m_l), and infinite (m_∞) sample sizes, respectively.

5.1 η - ϵ curves about data DB variability

According to Definition 5.1, the data DB variability degrades to the algorithm DB variability $AV(f_{\mathcal{Q}}, \mathcal{D})$ when $\mathcal{S}_\eta = \mathcal{S}$. In other words, the algorithm DB variability is a special case of the data DB variability with $\eta = 1$. Therefore, the data DB variability could present more detailed information on reflecting how the decision boundary variability depends on the training set, especially when we observe the variation of the reconstruction error ϵ *w.r.t.* different η .

To explore the relationship between the reconstruction error ϵ and the proportion of subset η , we train 1,000 networks of ResNet-18 on CIFAR-10 and CIFAR-100 of different sample sizes m . Albeit finding the most suitable η -subset is intractable, we adopt a coreset selection approach named, *selection via proxy* [9], which can rank the importance of training examples, to estimate the η -subset for a given training set \mathcal{S} and proportion η . Then, through repeatedly training the network on \mathcal{S}_η , we can estimate the reconstruction error ϵ . The η - ϵ curves of CIFAR-10 and CIFAR-100 are presented in Figure 6(a) and 6(b), respectively. From the plots, we have an observation that *there is a more rapid decline in ϵ along with small η* and also a smaller algorithm DB variability when the training sample size m is larger. Furthermore, we plot the schematic diagram of η - ϵ curves *w.r.t.* different sample size m , as shown in Figure 6(c). When $\eta = 0$, $f_{\mathcal{A}(\mathcal{S}_\eta)}$ cannot be better than random guess, and hence $\epsilon = \frac{k-1}{k}$, where k is the number of potential categories. It is worth noting that that ϵ has a sharper drop along with η when the sample size m is larger. Therefore, we rationally propose the following assumption, which is also shown by the right angle with m_∞ in Figure 6(c).

Assumption 5.2. If $m \rightarrow \infty$, we have $\epsilon \rightarrow 0$ when $\eta \rightarrow 0$.

These plots indicate that the area under the η - ϵ curve could be a more meticulous predictor for the generalization ability of neural networks compared to the algorithm DB variability, which is only a point on the η - ϵ curve when $\eta = 1$. Hence, the area under the η - ϵ curve can also be considered as an extension of the algorithm DB variability: if the Gibbs classifier $f_{\mathcal{A}(\mathcal{S})}$ possesses a smaller area under the η - ϵ curve, it produces more stable decision boundaries with varying training subsets.

5.2 Theoretical evidence

In this section, we develop the theoretical foundations for the data decision boundary variability. Our theory suggests that *neural networks with better data DB variability possess better generalization*, which fully supports our theory.

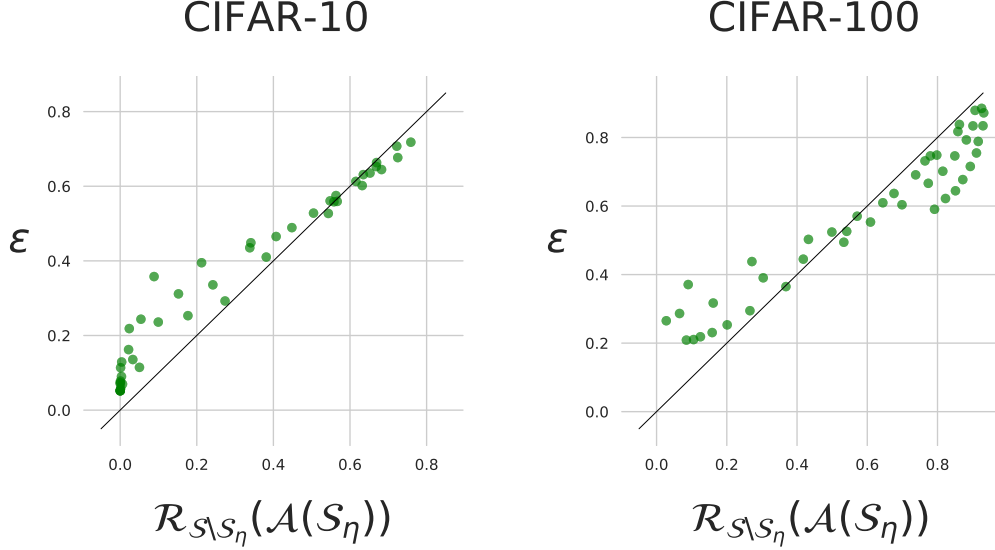


Figure 7: Scatter of ϵ (y -axis) and $\mathcal{R}_{\mathcal{S} \setminus \mathcal{S}_\eta}(\mathcal{A}(\mathcal{S}_\eta))$ (x -axis) on CIFAR-10 and CIFAR-100.

According to the definition of data decision boundary variability, the η -subset \mathcal{S}_η plays a similar role of “support vector set”, and the complement set $\mathcal{S} \setminus \mathcal{S}_\eta = \mathcal{S} - \mathcal{S}_\eta$ is supposed to be sampled from simpler distributions than \mathcal{D} . Therefore, we make the following mild assumption.

Assumption 5.3. Examples in $\mathcal{S} \setminus \mathcal{S}_\eta$ are assumed to be drawn from the distribution \mathcal{D}_1 , where for all $(\mathbf{x}, y) \sim \mathcal{D}_1$, $\mathbb{E}_{\boldsymbol{\theta} \sim \mathcal{A}(\mathcal{S}_\eta)}[\mathbb{I}(y \in T(f_{\boldsymbol{\theta}}, \mathbf{x}))] = \max_{i \in [k]} \mathbb{E}_{\boldsymbol{\theta} \sim \mathcal{A}(\mathcal{S}_\eta)}[\mathbb{I}(i \in T(f_{\boldsymbol{\theta}}, \mathbf{x}))]$ holds, and

$$\begin{aligned} & \mathbb{E}_{\mathcal{D}_1} \mathbb{E}_{\boldsymbol{\theta} \sim \mathcal{A}(\mathcal{S}), \boldsymbol{\theta}' \sim \mathcal{A}(\mathcal{S}_\eta)} [\mathbb{I}(T(f_{\boldsymbol{\theta}}, \mathbf{x}) \neq T(f_{\boldsymbol{\theta}'}, \mathbf{x}))] \\ & \leq \mathbb{E}_{\mathcal{D}} \mathbb{E}_{\boldsymbol{\theta} \sim \mathcal{A}(\mathcal{S}), \boldsymbol{\theta}' \sim \mathcal{A}(\mathcal{S}_\eta)} [\mathbb{I}(T(f_{\boldsymbol{\theta}}, \mathbf{x}) \neq T(f_{\boldsymbol{\theta}'}, \mathbf{x}))] = \epsilon \end{aligned}$$

Remark 5.4. Assumption 5.3 can also be stated as follows: the data (\mathcal{D}_1) correctly classified by $f_{\mathcal{A}(\mathcal{S}_\eta)}$ possesses a lower data decision boundary variability than the average data decision boundary variability on \mathcal{D} .

Given Assumption 5.3, we can further derive a probably approximately correct bound *w.r.t.* $\mathcal{R}_{\mathcal{S} \setminus \mathcal{S}_\eta}(\mathcal{A}(\mathcal{S}_\eta))$, as shown in the following lemma.

Lemma 5.5. *If the decision boundaries of $f_{\mathcal{A}(\mathcal{S})}$ possess a (ϵ, η) -data DB variability and Assumption 5.3 holds, then, with the probability of at least $1 - \delta$ over a sample of size m , we have*

$$\mathcal{R}_{\mathcal{S} \setminus \mathcal{S}_\eta}(\mathcal{A}(\mathcal{S}_\eta)) \leq \epsilon + \sqrt{\frac{1}{2(1-\eta)m} \log \frac{1}{\delta}}$$

We also conduct experiments to show the correlation between $\mathcal{R}_{\mathcal{S} \setminus \mathcal{S}_\eta}(\mathcal{A}(\mathcal{S}_\eta))$ and ϵ ; see Figure 7. From the plots we obtain an observation that $\mathcal{R}_{\mathcal{S} \setminus \mathcal{S}_\eta}(\mathcal{A}(\mathcal{S}_\eta)) \leq \epsilon$ is stable when $\mathcal{R}_{\mathcal{S} \setminus \mathcal{S}_\eta}(\mathcal{A}(\mathcal{S}_\eta))$ is small (about less than 0.5).

Lemma 5.6. *If the decision boundaries of $f_{\mathcal{A}(\mathcal{S})}$ possess a (ϵ, η) -data DB variability, then we have*

$$|\mathcal{R}_{\mathcal{D}}(\mathcal{A}(\mathcal{S})) - \mathcal{R}_{\mathcal{D}}(\mathcal{A}(\mathcal{S}_\eta))| \leq \epsilon.$$

Lemma 5.6 shows that the difference between the expected risk of $\mathcal{A}(\mathcal{S})$ and $\mathcal{A}(\mathcal{S}_\eta)$ can be bounded by their difference in decision boundaries. Then, we continue to prove the generalization bound with data decision boundary variability.

Theorem 5.7 (data DB variability-based upper bound on expected risk). *If the decision boundaries of $f_{\mathcal{A}(\mathcal{S})}$ possess a (ϵ, η) -data DB variability on the data generating distribution \mathcal{D} , and assume $\eta \leq 0.5$ and Assumption 5.3 holds, then, with the probability of at least $1 - \delta$ over a sample of size m , we have*

$$\mathcal{R}_{\mathcal{D}}(\mathcal{A}(\mathcal{S})) \leq \Omega + \sqrt{4\Omega\Delta} + 8\Delta + \epsilon, \quad (1)$$

where

$$\begin{aligned} \Omega &= \epsilon + \sqrt{\frac{1}{2(1-\eta)m} \log \frac{1}{\delta}}, \\ \Delta &= \eta \log \frac{e}{\eta} + \frac{1}{m} \log \frac{2}{\delta}. \end{aligned}$$

Moreover, for sufficient large m , we have

$$\mathcal{R}_{\mathcal{D}}(\mathcal{A}(\mathcal{S})) \leq \mathcal{O}\left(\frac{1}{\sqrt{m}} + \epsilon + \eta \log \frac{1}{\eta}\right). \quad (2)$$

According to Assumption 5.2, when $m \rightarrow \infty$, $\eta \rightarrow 0$ and $\epsilon \rightarrow 0$, while according to Eq. 2, $\mathcal{R}_{\mathcal{D}}(\mathcal{A}(\mathcal{S})) \rightarrow 0$. Therefore, the generalization bound is asymptotically converged. Theorem 5.7 suggests that a smaller data DB variability, corresponds to a tighter upper bound on the expected risk, which theoretically verifies the relationship between the data DB variability and the generalization ability of neural networks.

6 Discussions

This sections discusses how our findings would shed light on understanding other interesting phenomena.

6.1 Algorithm DB variability and the entropy of decision boundaries

If Assumption 4.3 holds for all $\theta \sim \mathbb{Q}$, $1 - AV(f_{\mathbb{Q}}, \mathcal{D})$ can be rewritten as

$$\mathbb{E}_{(\mathbf{x}, y) \sim \mathcal{D}} \sum_{i=1}^k \mathbb{E}_{\theta \sim \mathbb{Q}}^2 [\mathbb{I}(T(f_{\theta}, \mathbf{x}) = i)].$$

The term $\sum_{i=1}^k \mathbb{E}_{\theta \sim \mathbb{Q}}^2 [\mathbb{I}(T(f_{\theta}, \mathbf{x}) = i)]$ can be considered to measure the degree of prediction uncertainty for the given voxel \mathbf{x} in the input space \mathbb{R}^n . If we leverage $-\log(\cdot)$ on the term $\sum_{i=1}^k \mathbb{E}_{\theta \sim \mathbb{Q}}^2 [\mathbb{I}(T(f_{\theta}, \mathbf{x}) = i)]$, we have that

$$-\log \sum_{i=1}^k \mathbb{E}_{\theta \sim \mathbb{Q}}^2 [\mathbb{I}(T(f_{\theta}, \mathbf{x}) = i)],$$

denotes the collision entropy of prediction made by the Gibbs classifier $f_{\mathbb{Q}}$ on \mathbf{x} . We can also replace the collision entropy with canonical Shannon entropy,

$$-\sum_{i=1}^k \mathbb{E}_{\theta \sim \mathbb{Q}} [\mathbb{I}(T(f_{\theta}, \mathbf{x}) = i)] \log \mathbb{E}_{\theta \sim \mathbb{Q}} [\mathbb{I}(T(f_{\theta}, \mathbf{x}) = i)],$$

in the future research. As such, the algorithm DB variability is closely related to the “entropy of decision boundary”, and the uncanny generalization in neural networks might be further uncovered by investigating this low entropy of decision boundary.

6.2 Data DB variability and the complexity of DBs

According to the work by Guan and Loew [14], a complex decision boundary has large curvatures and conjectured to indicate inferior generalization. Nevertheless, from the perspective of causality, we argue that the large curvatures or the non-linearity of DBs *is the result other than the cause* for classification tasks, and the primary factor in shaping a complex DB during the training procedure should be the significant non-linearity of the training data. If only the geometric properties of decision boundaries are analysed without investigating the data, the results might be incomplete and even misleading. Another obstacle for describing the complexity of DBs by its geometric properties is the huge dimensional input space, which makes the geometric properties of DBs hard to quantify and estimate. Therefore, defining the complexity of DBs based on its curvature is not rational and impractical.

Here, we consider the complexity of DBs from the perspective of the training set. During the training procedure, a small part of training examples, considered as “support vectors”, play a more critical role in supervising the formation of decision boundaries and compelling the DB to be gradually more complicated. If the construction of decision boundaries relies on fewer “support vectors”, the decision boundary should be simpler. In other words, if these “support vectors” are excluded from the training sample, the DB will be notably dissimilar when the network is retrained on the modified training set. Hence, the complexity of DBs can be also defined with the notion of the data DB variability: *with (ϵ, η) -data decision boundary variability, the decision boundary of $f_{\mathcal{A}(\mathcal{S})}$ is said to possess a (ϵ, η) -complexity.*

By considering the data DB variability as the complexity of DB, many phenomenons *w.r.t.* generalization in deep learning can be easily understood: (1) difficult tasks generally have more complex decision boundaries, since their datum are more non-linear and contain more “support vectors”; (2) in adversarial training, each data point is converted to a “data ball” with the radius of the adversarial perturbation and has more impact on forming the DBs. Hence, adversarial training contributes to a more complex decision boundary by enlarging the “support vector set”, and thus causes the decline in generalization performance; (3) for data augmentation, generated images are also considered to obey the data generation distribution \mathcal{D} . Hence, data augmentation decreases the complexity of decision boundaries by greatly expanding the training set \mathcal{S} , while $|\mathcal{S}_\eta|$ has only a slight growth.

7 Experimental Implementation Details

This section provides all the additional implementation details for our experiments.

7.1 Model training

We employ SGD to optimize all the models and the momentum factor is 0.9. The weight decay factor is set to $5e-4$, and the learning rate is decayed by 0.2 every 50 epochs. Besides, basic data augmentation (crop and flip) [62] is adopted in both standard and adversarial training, and only the basic data augmentation is considered in our experiments and analysis.

Additional details in 4.1 We train VGG-16, ResNet-18, Wide-ResNet-28 on CIFAR-10 and CIFAR-100. In the training procedure, the model is trained for 200 epochs, in which the batch

size is set to 128, and the learning rate is initialized as 0.1. There are three training strategies included in this experiment: standard training, non-data-augmentation training, and adversarial training. In the adversarial training, the radius of the adversarial perturbation is set as $10/255$ and l_∞ distance is selected. The basic data augmentation (cropping and flipping) in the standard training and adversarial training is achieved by the following Pytorch code:

```
1 transforms.RandomCrop(32, padding=4)
2 transforms.RandomHorizontalFlip()
```

The experiment is repeated for 10 trials for each (dataset, architecture, training strategy) setting.

Additional details in 4.2 We repeatedly train 10 ResNet-18 on CIFAR-10 and CIFAR-100, respectively, with different random seeds. In the training procedure, the model is trained for 200 epochs, in which the batch size is set to 128, and the learning rate is initialized as 0.1 and 0.01, respectively. Basic data augmentation is included during the training process.

Additional details in 4.3 We randomly sample examples from the training set of CIFAR-10 and CIFAR-100 to form five datasets with different sizes of [2000, 5000, 10000, 20000, 50000], respectively. 10 ResNet-18 are trained for each dataset. In the training procedure, the model is trained for 200 epochs, in which the batch size is set to 128, and the learning rate is initialized as 0.1. Basic data augmentation is included during the training process.

Additional details in 4.4 We randomly change the labels of 20% examples in the training set of CIFAR-10 and CIFAR-100. Then, 10 ResNet-18 are optimize by SGD for 500 epochs on the noise CIFAR-10 and CIFAR-100, respectively. the momentum factor is 0.9, and the learning rate is 0.001 and does not decay during the training process.

Additional details in 4.5 We repeatedly train 10 VGG-16, ResNet-18, Wide-ResNet-28 on CIFAR-10 on the synthetic binary CIFAR-10 and CIFAR-100 (Figure 5(a)), respectively, with different random seeds. In the training procedure, the model is trained for 30 epochs, in which the batch size is set to 128, and the learning rate is fixed as 0.01, respectively. There is no data augmentation during the training process to preserve the location information of the feature in the synthetic images.

Additional details in 5.1 We randomly sample examples from the training set of CIFAR-10 and CIFAR-100 to form five datasets with different sizes of [2000, 5000, 10000, 20000, 50000], respectively. For each dataset, we obtain 10 η -subsets with different η of [0.1, 0.2, 0.3, 0.4, 0.5, 0.6, 0.7, 0.8, 0.9, 1.0] via a coreset selection approach named *selection via proxy* [9]. The related code can be downloaded from <https://github.com/stanford-futuredata/selection-via-proxy>. The ResNet-18 is repeatedly trained for 10 trials to estimate the complexity of decision boundaries for each η -subset.

8 Proofs

The section collects detailed proofs of the results that are omitted in Section 4.6 and 5.2. To avoid technicalities, the measurability/integrability issues are ignored throughout this paper. Moreover, Fubini’s theorem is assumed to be applicable for any integration *w.r.t.* multiple variables. In other words, the order of integrations is exchangeable.

8.1 Proof of Theorem 4.5

Proof. If Assumption 4.3 holds for all $\theta \sim \mathbb{Q}$, we have

$$\mathbb{E}_{(\mathbf{x}, y) \sim \mathcal{D}} \mathbb{E}_{\theta, \theta' \sim \mathbb{Q}} [\mathbb{I}(y \in T(f_\theta, \mathbf{x})) \mathbb{I}(y \in T(f_{\theta'}, \mathbf{x})) \mathbb{I}(T(f_\theta, \mathbf{x}) \neq T(f_{\theta'}, \mathbf{x}))] = 0$$

Hence,

$$\begin{aligned}
AV(f_{\mathbb{Q}}, \mathcal{D}) &= \mathbb{E}_{(\mathbf{x}, y) \sim \mathcal{D}} \mathbb{E}_{\boldsymbol{\theta}, \boldsymbol{\theta}' \sim \mathbb{Q}} [\mathbb{I}(T(f_{\boldsymbol{\theta}}, \mathbf{x}) \neq T(f_{\boldsymbol{\theta}'}, \mathbf{x}))] \\
&= \mathbb{E}_{(\mathbf{x}, y) \sim \mathcal{D}} \mathbb{E}_{\boldsymbol{\theta}, \boldsymbol{\theta}' \sim \mathbb{Q}} [\mathbb{I}(y \in T(f_{\boldsymbol{\theta}}, \mathbf{x})) \mathbb{I}(y \notin T(f_{\boldsymbol{\theta}'}, \mathbf{x})) \\
&\quad + \mathbb{I}(y \notin T(f_{\boldsymbol{\theta}}, \mathbf{x})) \mathbb{I}(T(f_{\boldsymbol{\theta}}, \mathbf{x}) \neq T(f_{\boldsymbol{\theta}'}, \mathbf{x}))] \\
&\leq 2\mathcal{R}_{\mathcal{D}}(\mathbb{Q})
\end{aligned} \tag{3}$$

The proof is completed. \square

8.2 Proof of Theorem 4.6

Proof. When the classification is binary, *i.e.*, $k = 2$, with Assumption 4.3, we have

$$\begin{aligned}
&\mathbb{E}_{(\mathbf{x}, y) \sim \mathcal{D}} \mathbb{E}_{\boldsymbol{\theta}, \boldsymbol{\theta}' \sim \mathbb{Q}} [\mathbb{I}(T(f_{\boldsymbol{\theta}}, \mathbf{x}) = T(f_{\boldsymbol{\theta}'}, \mathbf{x}))] \\
&= \mathbb{E}_{(\mathbf{x}, y) \sim \mathcal{D}} \mathbb{E}_{\boldsymbol{\theta} \sim \mathbb{Q}}^2 [\mathbb{I}(y \in T(f_{\boldsymbol{\theta}}, \mathbf{x}))] + \mathbb{E}_{(\mathbf{x}, y) \sim \mathcal{D}} \mathbb{E}_{\boldsymbol{\theta} \sim \mathbb{Q}}^2 [\mathbb{I}(y \notin T(f_{\boldsymbol{\theta}}, \mathbf{x}))] \\
&= \mathbb{E}_{(\mathbf{x}, y) \sim \mathcal{D}} \mathbb{E}_{\boldsymbol{\theta} \sim \mathbb{Q}}^2 [\mathbb{I}(y \in T(f_{\boldsymbol{\theta}}, \mathbf{x}))] + \mathbb{E}_{(\mathbf{x}, y) \sim \mathcal{D}} [1 - \mathbb{E}_{\boldsymbol{\theta} \sim \mathbb{Q}} [\mathbb{I}(y \in T(f_{\boldsymbol{\theta}}, \mathbf{x}))]]^2 \\
&= 2\mathbb{E}_{(\mathbf{x}, y) \sim \mathcal{D}} \mathbb{E}_{\boldsymbol{\theta} \sim \mathbb{Q}}^2 [\mathbb{I}(y \in T(f_{\boldsymbol{\theta}}, \mathbf{x}))] + 2\mathcal{R}_{\mathcal{D}}(\mathbb{Q}) - 1
\end{aligned}$$

Plugging in $\text{Var}_{(\mathbf{x}, y) \sim \mathcal{D}} [\mathbb{E}_{\boldsymbol{\theta} \sim \mathbb{Q}} [\mathbb{I}(y \in T(f_{\boldsymbol{\theta}}, \mathbf{x}))]] = \mathbb{E}_{(\mathbf{x}, y) \sim \mathcal{D}} \mathbb{E}_{\boldsymbol{\theta} \sim \mathbb{Q}}^2 [\mathbb{I}(y \in T(f_{\boldsymbol{\theta}}, \mathbf{x}))] - (1 - \mathcal{R}_{\mathcal{D}}(\mathbb{Q}))^2$ yields

$$\begin{aligned}
&\mathbb{E}_{(\mathbf{x}, y) \sim \mathcal{D}} \mathbb{E}_{\boldsymbol{\theta}, \boldsymbol{\theta}' \sim \mathbb{Q}} [\mathbb{I}(T(f_{\boldsymbol{\theta}}, \mathbf{x}) = T(f_{\boldsymbol{\theta}'}, \mathbf{x}))] \\
&= 2 \text{Var}_{(\mathbf{x}, y) \sim \mathcal{D}} [\mathbb{E}_{\boldsymbol{\theta} \sim \mathbb{Q}} [\mathbb{I}(y \in T(f_{\boldsymbol{\theta}}, \mathbf{x}))]] + \mathcal{R}_{\mathcal{D}}^2(\mathbb{Q}) + (1 - \mathcal{R}_{\mathcal{D}}(\mathbb{Q}))^2 \\
&\geq \mathcal{R}_{\mathcal{D}}^2(\mathbb{Q}) + (1 - \mathcal{R}_{\mathcal{D}}(\mathbb{Q}))^2
\end{aligned}$$

Plugging in $\mathbb{E}_{(\mathbf{x}, y) \sim \mathcal{D}} \mathbb{E}_{\boldsymbol{\theta}, \boldsymbol{\theta}' \sim \mathbb{Q}} [\mathbb{I}(T(f_{\boldsymbol{\theta}}, \mathbf{x}) = T(f_{\boldsymbol{\theta}'}, \mathbf{x}))] = 1 - AV(f_{\mathbb{Q}}, \mathcal{D})$ and solving the inequality yield the desired inequality and finishes the proof of Theorem 4.6. \square

8.3 Proof of Lemma 5.5

Proof. According to Assumption 5.3 that for all $(\mathbf{x}, y) \sim \mathcal{D}_1$, we have

$$\mathbb{E}_{\boldsymbol{\theta} \sim \mathcal{A}(\mathcal{S}_{\eta})} [\mathbb{I}(y \in T(f_{\boldsymbol{\theta}}, \mathbf{x}))] = \max_{i \in [k]} \mathbb{E}_{\boldsymbol{\theta} \sim \mathcal{A}(\mathcal{S}_{\eta})} [\mathbb{I}(i \in T(f_{\boldsymbol{\theta}}, \mathbf{x}))],$$

then

$$\begin{aligned}
&\mathcal{R}_{\mathcal{D}_1}(\mathcal{A}(\mathcal{S}_{\eta})) \\
&= 1 - \mathbb{E}_{(\mathbf{x}, y) \sim \mathcal{D}_1} \mathbb{E}_{\boldsymbol{\theta} \sim \mathcal{A}(\mathcal{S}_{\eta})} [\mathbb{I}(y = T(f_{\boldsymbol{\theta}}, \mathbf{x}))] \\
&= 1 - \mathbb{E}_{\mathcal{D}_1} \sum_{i=1}^k \mathbb{E}_{\mathcal{A}(\mathcal{S})} [\mathbb{I}(i = T(f_{\boldsymbol{\theta}}, \mathbf{x}))] \mathbb{E}_{\mathcal{A}(\mathcal{S}_{\eta})} [\mathbb{I}(y = T(f_{\boldsymbol{\theta}}, \mathbf{x}))] \\
&\leq 1 - \mathbb{E}_{\mathcal{D}_1} \sum_{i=1}^k \mathbb{E}_{\mathcal{A}(\mathcal{S})} [\mathbb{I}(i = T(f_{\boldsymbol{\theta}}, \mathbf{x}))] \mathbb{E}_{\mathcal{A}(\mathcal{S}_{\eta})} [\mathbb{I}(i = T(f_{\boldsymbol{\theta}}, \mathbf{x}))] \\
&= \mathbb{E}_{\mathcal{D}_1} \mathbb{E}_{\boldsymbol{\theta} \sim \mathcal{A}(\mathcal{S}), \boldsymbol{\theta}' \sim \mathcal{A}(\mathcal{S}_{\eta})} [\mathbb{I}(T(f_{\boldsymbol{\theta}}, \mathbf{x}) \neq T(f_{\boldsymbol{\theta}'}, \mathbf{x}))] \\
&\leq \mathbb{E}_{\mathcal{D}} \mathbb{E}_{\boldsymbol{\theta} \sim \mathcal{A}(\mathcal{S}), \boldsymbol{\theta}' \sim \mathcal{A}(\mathcal{S}_{\eta})} [\mathbb{I}(T(f_{\boldsymbol{\theta}}, \mathbf{x}) \neq T(f_{\boldsymbol{\theta}'}, \mathbf{x}))] \\
&= \epsilon.
\end{aligned}$$

Because the examples in $\mathcal{S} \setminus \mathcal{S}_\eta$ are drawn from \mathcal{D}_1 , by applying Hoeffding's Inequality, we have

$$\Pr [\mathcal{R}_{\mathcal{S} \setminus \mathcal{S}_\eta} - \mathcal{R}_{\mathcal{D}_1} \geq t] \leq \exp(-2(1 - \eta)mt^2). \quad (4)$$

Plug in $\delta = \exp(-2(1 - \eta)mt^2)$ into Eq. 4, thus, with the probability of at least $1 - \delta$, we have

$$\mathcal{R}_{\mathcal{S} \setminus \mathcal{S}_\eta}(\mathcal{A}(\mathcal{S}_\eta)) \leq \epsilon + \sqrt{\frac{1}{2(1 - \eta)m} \log \frac{1}{\delta}}.$$

□

8.4 Proof of Lemma 5.6

Proof. From the definition of data DB variability, there exists a η -subset \mathcal{S}_η s.t.

$$\mathbb{E}_{(\mathbf{x}, y) \sim \mathcal{D}} \mathbb{E}_{\boldsymbol{\theta} \sim \mathcal{A}(\mathcal{S}), \boldsymbol{\theta}' \sim \mathcal{A}(\mathcal{S}_\eta)} [\mathbb{I}(T(\mathbf{f}_\boldsymbol{\theta}, \mathbf{x}) \neq T(\mathbf{f}_{\boldsymbol{\theta}'}, \mathbf{x}))] = \epsilon.$$

Recall the LHS = $|\mathcal{R}_{\mathcal{D}}(\mathcal{A}(\mathcal{S})) - \mathcal{R}_{\mathcal{D}}(\mathcal{A}(\mathcal{S}_\eta))|$ and denote $\mathbb{E}_{(\mathbf{x}, y) \sim \mathcal{D}} \mathbb{E}_{\boldsymbol{\theta} \sim \mathcal{A}(\mathcal{S}), \boldsymbol{\theta}' \sim \mathcal{A}(\mathcal{S}_\eta)}$ as $\mathbb{E}_{\mathcal{D}, \mathcal{A}(\mathcal{S}), \mathcal{A}(\mathcal{S}_\eta)}$ for simplicity, then

$$\begin{aligned} \text{LHS} &= \left| \mathbb{E}_{(\mathbf{x}, y) \sim \mathcal{D}} \mathbb{E}_{\boldsymbol{\theta} \sim \mathcal{A}(\mathcal{S})} [\mathbb{I}(y \notin T(\mathbf{f}_\boldsymbol{\theta}, \mathbf{x}))] - \mathbb{E}_{(\mathbf{x}, y) \sim \mathcal{D}} \mathbb{E}_{\boldsymbol{\theta} \sim \mathcal{A}(\mathcal{S}_\eta)} [\mathbb{I}(y \notin T(\mathbf{f}_\boldsymbol{\theta}, \mathbf{x}))] \right| \\ &= \left| \mathbb{E}_{\mathcal{D}, \mathcal{A}(\mathcal{S}), \mathcal{A}(\mathcal{S}_\eta)} [\mathbb{I}(y \notin T(\mathbf{f}_\boldsymbol{\theta}, \mathbf{x})) - \mathbb{I}(y \notin T(\mathbf{f}_{\boldsymbol{\theta}'}, \mathbf{x}))] \right| \\ &\leq \mathbb{E}_{\mathcal{D}, \mathcal{A}(\mathcal{S}), \mathcal{A}(\mathcal{S}_\eta)} [|\mathbb{I}(y \notin T(\mathbf{f}_\boldsymbol{\theta}, \mathbf{x})) - \mathbb{I}(y \notin T(\mathbf{f}_{\boldsymbol{\theta}'}, \mathbf{x}))|] \\ &\leq \mathbb{E}_{\mathcal{D}, \mathcal{A}(\mathcal{S}), \mathcal{A}(\mathcal{S}_\eta)} [\mathbb{I}(T(\mathbf{f}_\boldsymbol{\theta}, \mathbf{x}) \neq T(\mathbf{f}_{\boldsymbol{\theta}'}, \mathbf{x}))] = \epsilon \end{aligned}$$

The proof is completed. □

8.5 Proof of Theorem 5.7

We first introduce Lemma 8.1 and Lemma 8.2 as below.

Lemma 8.1 (Lemma 30.1 in [50]). *Assume T and V are two datasets independently sampled from the data generating distribution \mathcal{D} , then, with the probability of at least $1 - \delta$, we have*

$$\mathcal{R}_{\mathcal{D}}(\mathcal{A}(T)) \leq \mathcal{R}_V(\mathcal{A}(T)) + \sqrt{\frac{2\mathcal{R}_V(\mathcal{A}(T)) \log(1/\delta)}{|V|}} + \frac{4 \log(1/\delta)}{|V|}.$$

Lemma 8.2 (Theorem 30.2 in [50]). *Let \mathcal{S}_η be a η -subset of the dataset \mathcal{S} , which is sampled from the data generation distribution \mathcal{D} and the sample size $|\mathcal{S}| = m$. Let $\mathcal{S} \setminus \mathcal{S}_\eta = \mathcal{S} - \mathcal{S}_\eta$ and assume $\eta \leq 0.5$. Then, with the probability of at least $1 - \delta$ over a sample of size m , we have*

$$\mathcal{R}_{\mathcal{D}}(\mathcal{A}(\mathcal{S}_\eta)) \leq \mathcal{R}_{\mathcal{S} \setminus \mathcal{S}_\eta}(\mathcal{A}(\mathcal{S}_\eta)) + \sqrt{4\mathcal{R}_{\mathcal{S} \setminus \mathcal{S}_\eta}(\mathcal{A}(\mathcal{S}_\eta))\Delta} + 8\Delta,$$

where

$$\Delta = \eta \log \frac{e}{\eta} + \frac{1}{m} \log \frac{1}{\delta}.$$

Proof of Lemma 8.2.

$$\begin{aligned}
& \Pr \left[\exists \mathcal{S}_\eta \subseteq \mathcal{S} \text{ s.t. } \mathcal{R}_{\mathcal{D}}(\mathcal{A}(\mathcal{S}_\eta)) \leq \mathcal{R}_{\mathcal{S} \setminus \mathcal{S}_\eta}(\mathcal{A}(\mathcal{S}_\eta)) + \sqrt{\frac{2\mathcal{R}_{\mathcal{S} \setminus \mathcal{S}_\eta}(\mathcal{A}(\mathcal{S}_\eta)) \log(1/\delta)}{|\mathcal{S} \setminus \mathcal{S}_\eta|}} + \frac{4 \log(1/\delta)}{|\mathcal{S} \setminus \mathcal{S}_\eta|} \right] \\
& \leq \sum_{\mathcal{S}_\eta \subseteq \mathcal{S}} \Pr \left[\mathcal{R}_{\mathcal{D}}(\mathcal{A}(\mathcal{S}_\eta)) \leq \mathcal{R}_{\mathcal{S} \setminus \mathcal{S}_\eta}(\mathcal{A}(\mathcal{S}_\eta)) + \sqrt{\frac{2\mathcal{R}_{\mathcal{S} \setminus \mathcal{S}_\eta}(\mathcal{A}(\mathcal{S}_\eta)) \log(1/\delta)}{|\mathcal{S} \setminus \mathcal{S}_\eta|}} + \frac{4 \log(1/\delta)}{|\mathcal{S} \setminus \mathcal{S}_\eta|} \right] \\
& = \binom{m}{\eta m} \delta \leq \left(\frac{e}{\eta} \right)^{\eta m} \delta
\end{aligned}$$

Plug in $\delta' = \left(\frac{e}{\eta} \right)^{\eta m} \delta$, and use the assumption $\eta \leq \frac{1}{2}$, which implies $|\mathcal{S} \setminus \mathcal{S}_\eta| \geq \frac{m}{2}$, then, with the probability of at least $1 - \delta'$, we have that

$$\mathcal{R}_{\mathcal{D}}(\mathcal{A}(\mathcal{S}_\eta)) \leq \mathcal{R}_{\mathcal{S} \setminus \mathcal{S}_\eta}(\mathcal{A}(\mathcal{S}_\eta)) + \sqrt{4\mathcal{R}_{\mathcal{S} \setminus \mathcal{S}_\eta}(\mathcal{A}(\mathcal{S}_\eta)) \left(\eta \log \frac{e}{\eta} + \frac{1}{m} \log \frac{1}{\delta'} \right)} + 8 \left(\eta \log \frac{e}{\eta} + \frac{1}{m} \log \frac{1}{\delta'} \right),$$

which concludes the proof. \square

With the above lemmas, we can derive the generalization bound based on the complexity of decision boundary.

Proof of Theorem 5.7. According to Lemma 8.2, with the probability of at least $1 - \delta$, we have

$$\mathcal{R}_{\mathcal{S} \setminus \mathcal{S}_\eta}(\mathcal{A}(\mathcal{S}_\eta)) \leq \epsilon + \sqrt{\frac{1}{2(1-\eta)m} \log \frac{1}{\delta}}.$$

Through combining this with Lemma 8.2, with the probability of at least $1 - 2\delta$, we have

$$\mathcal{R}_{\mathcal{D}}(\mathcal{A}(\mathcal{S}_\eta)) \leq \Omega + \sqrt{4\Omega\Delta} + 8\Delta, \tag{5}$$

where

$$\begin{aligned}
\Omega &= \epsilon + \sqrt{\frac{1}{2(1-\eta)m} \log \frac{1}{\delta}}, \\
\Delta &= \eta \log \frac{e}{\eta} + \frac{1}{m} \log \frac{1}{\delta}.
\end{aligned}$$

Plugging the equality of $\mathcal{R}_{\mathcal{D}}(\mathcal{A}(\mathcal{S})) \leq \mathcal{R}_{\mathcal{D}}(\mathcal{A}(\mathcal{S}_\eta)) + \epsilon$ in Lemma 5.6 into Eq. 5 yields the desired inequality of Eq. 1.

When m is sufficient large, $\sqrt{4\Omega\Delta}$ can be dropped due to $\sqrt{4\Omega\Delta} \leq \Omega + \Delta$. Considering $\eta \leq 0.5$, $\Omega \leq \sqrt{\frac{1}{2m} \log \frac{1}{\delta}} + \epsilon = \mathcal{O}\left(\frac{1}{\sqrt{m}} + \epsilon\right)$. The term $\frac{1}{m} \log \frac{1}{\delta}$ in Δ can be dropped because it has a faster convergence speed compared to $\sqrt{\frac{1}{2m} \log \frac{1}{\delta}}$ in Ω . Because $\log \frac{1}{\delta}$ is considered as a constant, we have

$$\mathcal{R}_{\mathcal{D}}(\mathcal{A}(\mathcal{S})) \leq \mathcal{O}\left(\frac{1}{\sqrt{m}} + \epsilon + \eta \log \frac{1}{\eta}\right).$$

The proof of Theorem 5.7 is finished. \square

9 Conclusion

In this paper, we empirically and theoretically explored the relationship between decision boundary variability and generalization in neural networks, through the notions of algorithm DB variability and data DB variability, respectively. A significant negative correlation between the decision boundary variability and generalization performance is observed in our experiments. As for the theoretical results, two lower bounds based on algorithm DB variability and an upper bound based on data DB variability are proposed, respectively, for the sake of enhancing our findings.

References

- [1] Motasem Alfarra, Adel Bibi, Hasan Hammoud, Mohamed Gaafar, and Bernard Ghanem. On the decision boundaries of deep neural networks: A tropical geometry perspective, 2020. URL <https://openreview.net/forum?id=By11dnNFwS>.
- [2] Peter L Bartlett and Shahar Mendelson. Rademacher and gaussian complexities: Risk bounds and structural results. *Journal of Machine Learning Research*, 3(Nov):463–482, 2002.
- [3] Mikhail Belkin, Daniel Hsu, Siyuan Ma, and Soumik Mandal. Reconciling modern machine-learning practice and the classical bias–variance trade-off. *Proceedings of the National Academy of Sciences*, 116(32):15849–15854, 2019.
- [4] Léon Bottou. Large-scale machine learning with stochastic gradient descent. In *Proceedings of COMPSTAT’2010*, pages 177–186. Springer, 2010.
- [5] Tom Brown, Benjamin Mann, Nick Ryder, Melanie Subbiah, Jared D Kaplan, Prafulla Dhariwal, Arvind Neelakantan, Pranav Shyam, Girish Sastry, Amanda Askell, et al. Language models are few-shot learners. *Advances in neural information processing systems*, 33:1877–1901, 2020.
- [6] Nicholas Carlini and David Wagner. Towards evaluating the robustness of neural networks. In *2017 IEEE Symposium on Security and Privacy (SP)*, pages 39–57. IEEE, 2017.
- [7] Zhaohui Che, Ali Borji, Guangtao Zhai, Suiyi Ling, Jing Li, Xiongkuo Min, Guodong Guo, and Patrick Le Callet. Smgea: A new ensemble adversarial attack powered by long-term gradient memories. *IEEE Transactions on Neural Networks and Learning Systems*, 33(3):1051–1065, 2022. doi: 10.1109/TNNLS.2020.3039295.
- [8] Lenaic Chizat and Francis Bach. Implicit bias of gradient descent for wide two-layer neural networks trained with the logistic loss. In *Conference on Learning Theory*, pages 1305–1338. PMLR, 2020.
- [9] Cody Coleman, Christopher Yeh, Stephen Mussmann, Baharan Mirzasoleiman, Peter Bailis, Percy Liang, Jure Leskovec, and Matei Zaharia. Selection via proxy: Efficient data selection for deep learning. In *International Conference on Learning Representations*, 2020. URL <https://openreview.net/forum?id=HJg2b0VYDr>.
- [10] Cong Fang, Hangfeng He, Qi Long, and Weijie J Su. Exploring deep neural networks via layer-peeled model: Minority collapse in imbalanced training. *Proceedings of the National Academy of Sciences*, 118(43), 2021.
- [11] Stanislav Fort, Paweł Krzysztof Nowak, Stanisław Jastrzebski, and Srinivasa Narayanan. Stiffness: A new perspective on generalization in neural networks. *arXiv preprint arXiv:1901.09491*, 2019.

- [12] Micah Goldblum, Jonas Geiping, Avi Schwarzschild, Michael Moeller, and Tom Goldstein. Truth or backpropaganda? an empirical investigation of deep learning theory. In *International Conference on Learning Representations*, 2020.
- [13] Ian J Goodfellow, Jonathon Shlens, and Christian Szegedy. Explaining and harnessing adversarial examples. *arXiv preprint arXiv:1412.6572*, 2014.
- [14] Shuyue Guan and Murray Loew. Analysis of generalizability of deep neural networks based on the complexity of decision boundary. In *2020 19th IEEE International Conference on Machine Learning and Applications (ICMLA)*, pages 101–106. IEEE, 2020.
- [15] Moritz Hardt, Ben Recht, and Yoram Singer. Train faster, generalize better: Stability of stochastic gradient descent. In *International Conference on Machine Learning*, pages 1225–1234. PMLR, 2016.
- [16] Fengxiang He and Dacheng Tao. Recent advances in deep learning theory. *arXiv preprint arXiv:2012.10931*, 2020.
- [17] Fengxiang He, Tongliang Liu, and Dacheng Tao. Control batch size and learning rate to generalize well: Theoretical and empirical evidence. In *Advances in Neural Information Processing Systems*, pages 1143–1152, 2019.
- [18] Fengxiang He, Bohan Wang, and Dacheng Tao. Piecewise linear activations substantially shape the loss surfaces of neural networks. In *International Conference on Learning Representations*, 2020.
- [19] Hangfeng He and Weijie Su. The local elasticity of neural networks. In *International Conference on Learning Representations*, 2020.
- [20] Kaiming He, Xiangyu Zhang, Shaoqing Ren, and Jian Sun. Deep residual learning for image recognition. In *Proceedings of the IEEE conference on computer vision and pattern recognition*, pages 770–778, 2016.
- [21] Warren He, Bo Li, and Dawn Song. Decision boundary analysis of adversarial examples. In *International Conference on Learning Representations*, 2018.
- [22] Qiang Hu, Hao Zhang, Feifei Gao, Chengwen Xing, and Jianping An. Analysis on the number of linear regions of piecewise linear neural networks. *IEEE Transactions on Neural Networks and Learning Systems*, 33(2):644–653, 2022. doi: 10.1109/TNNLS.2020.3028431.
- [23] Ziwei Ji and Matus Telgarsky. Directional convergence and alignment in deep learning. In H. Larochelle, M. Ranzato, R. Hadsell, M. F. Balcan, and H. Lin, editors, *Advances in Neural Information Processing Systems*, volume 33, pages 17176–17186. Curran Associates, Inc., 2020. URL <https://proceedings.neurips.cc/paper/2020/file/c76e4b2fa54f8506719a5c0dc14c2eb9-Paper.pdf>.
- [24] Yiding Jiang, Vaishnavh Nagarajan, Christina Baek, and J Zico Kolter. Assessing generalization of sgd via disagreement. *arXiv preprint arXiv:2106.13799*, 2021.
- [25] Chi Jin, Rong Ge, Praneeth Netrapalli, Sham M Kakade, and Michael I Jordan. How to escape saddle points efficiently. In *International Conference on Machine Learning*, pages 1724–1732. PMLR, 2017.

- [26] Dimitris Kalimeris, Gal Kaplun, Preetum Nakkiran, Benjamin Edelman, Tristan Yang, Boaz Barak, and Haofeng Zhang. Sgd on neural networks learns functions of increasing complexity. *Advances in Neural Information Processing Systems*, 32:3496–3506, 2019.
- [27] Hamid Karimi and Jiliang Tang. Decision boundary of deep neural networks: Challenges and opportunities. In *Proceedings of the 13th International Conference on Web Search and Data Mining*, pages 919–920, 2020.
- [28] Hamid Karimi, Tyler Derr, and Jiliang Tang. Characterizing the decision boundary of deep neural networks. *arXiv preprint arXiv:1912.11460*, 2019.
- [29] Kenji Kawaguchi. Deep learning without poor local minima. In *Advances in Neural Information Processing Systems*, 2016.
- [30] A. Krizhevsky and G. Hinton. Learning multiple layers of features from tiny images. *Master’s thesis, Department of Computer Science, University of Toronto*, 2009.
- [31] Alex Krizhevsky, Ilya Sutskever, and Geoffrey E Hinton. Imagenet classification with deep convolutional neural networks. *Advances in neural information processing systems*, 25:1097–1105, 2012.
- [32] Zhu Li, Weijie Su, and Dino Sejdinovic. Benign overfitting and noisy features. *arXiv preprint arXiv:2008.02901*, 2020.
- [33] Jian Liu, Naveed Akhtar, and Ajmal Mian. Adversarial attack on skeleton-based human action recognition. *IEEE Transactions on Neural Networks and Learning Systems*, 33(4):1609–1622, 2022. doi: 10.1109/TNNLS.2020.3043002.
- [34] Haihao Lu and Kenji Kawaguchi. Depth creates no bad local minima. *arXiv preprint arXiv:1702.08580*, 2017.
- [35] Scott M Lundberg and Su-In Lee. A unified approach to interpreting model predictions. In I. Guyon, U. V. Luxburg, S. Bengio, H. Wallach, R. Fergus, S. Vishwanathan, and R. Garnett, editors, *Advances in Neural Information Processing Systems 30*, pages 4765–4774. Curran Associates, Inc., 2017. URL <http://papers.nips.cc/paper/7062-a-unified-approach-to-interpreting-model-predictions.pdf>.
- [36] Kaifeng Lyu and Jian Li. Gradient descent maximizes the margin of homogeneous neural networks. In *International Conference on Learning Representations*, 2020. URL <https://openreview.net/forum?id=SJeLIgBKPS>.
- [37] Chao Ma, Stephan Wojtowytsch, Lei Wu, et al. Towards a mathematical understanding of neural network-based machine learning: what we know and what we don’t. *arXiv preprint arXiv:2009.10713*, 2020.
- [38] Aleksander Madry, Aleksandar Makelov, Ludwig Schmidt, Dimitris Tsipras, and Adrian Vladu. Towards deep learning models resistant to adversarial attacks. *arXiv preprint arXiv:1706.06083*, 2017.
- [39] Aleksander Madry, Aleksandar Makelov, Ludwig Schmidt, Dimitris Tsipras, and Adrian Vladu. Towards deep learning models resistant to adversarial attacks. In *International Conference on Learning Representations*, 2018.

- [40] David Mickisch, Felix Assion, Florens Grefßner, Wiebke Günther, and Mariele Motta. Understanding the decision boundary of deep neural networks: An empirical study. *arXiv preprint arXiv:2002.01810*, 2020.
- [41] Mehryar Mohri, Afshin Rostamizadeh, and Ameet Talwalkar. *Foundations of machine learning*. MIT press, 2018.
- [42] Preetum Nakkiran, Gal Kaplun, Yamini Bansal, Tristan Yang, Boaz Barak, and Ilya Sutskever. Deep double descent: Where bigger models and more data hurt. *arXiv preprint arXiv:1912.02292*, 2019.
- [43] Preetum Nakkiran, Behnam Neyshabur, and Hanie Sedghi. The deep bootstrap framework: Good online learners are good offline generalizers. *arXiv preprint arXiv:2010.08127*, 2020.
- [44] Guillermo Ortiz-Jimenez, Apostolos Modas, Seyed-Mohsen Moosavi-Dezfooli, and Pascal Frossard. Hold me tight! influence of discriminative features on deep network boundaries. *arXiv preprint arXiv:2002.06349*, 2020.
- [45] Vardan Papyan, XY Han, and David L Donoho. Prevalence of neural collapse during the terminal phase of deep learning training. *Proceedings of the National Academy of Sciences*, 117(40):24652–24663, 2020.
- [46] Yifan Qian, Paul Expert, Tom Rieu, Pietro Panzarasa, and Mauricio Barahona. Quantifying the alignment of graph and features in deep learning. *IEEE Transactions on Neural Networks and Learning Systems*, 33(4):1663–1672, 2022. doi: 10.1109/TNNLS.2020.3043196.
- [47] Nasim Rahaman, Aristide Baratin, Devansh Arpit, Felix Draxler, Min Lin, Fred Hamprecht, Yoshua Bengio, and Aaron Courville. On the spectral bias of neural networks. In *International Conference on Machine Learning*, pages 5301–5310. PMLR, 2019.
- [48] Pouya Samangouei, Ardavan Saeedi, Liam Nakagawa, and Nathan Silberman. Explaining: Model explanation via decision boundary crossing transformations. In *Proceedings of the European Conference on Computer Vision (ECCV)*, pages 666–681, 2018.
- [49] Harshay Shah, Kaustav Tamuly, Aditi Raghunathan, Prateek Jain, and Praneeth Netrapalli. The pitfalls of simplicity bias in neural networks. *arXiv preprint arXiv:2006.07710*, 2020.
- [50] Shai Shalev-Shwartz and Shai Ben-David. *Understanding machine learning: From theory to algorithms*. Cambridge university press, 2014.
- [51] Lloyd S Shapley. Notes on the n-person game—ii: The value of an n-person game.(1951). 1951.
- [52] Karen Simonyan and Andrew Zisserman. Very deep convolutional networks for large-scale image recognition. *arXiv preprint arXiv:1409.1556*, 2014.
- [53] Daniel Soudry, Elad Hoffer, Mor Shpigel Nacson, Suriya Gunasekar, and Nathan Srebro. The implicit bias of gradient descent on separable data. *The Journal of Machine Learning Research*, 19(1):2822–2878, 2018.
- [54] Dong Su, Huan Zhang, Hongge Chen, Jinfeng Yi, Pin-Yu Chen, and Yupeng Gao. Is robustness the cost of accuracy?—a comprehensive study on the robustness of 18 deep image classification models. In *Proceedings of the European Conference on Computer Vision (ECCV)*, pages 631–648, 2018.

- [55] Christian Szegedy, Wojciech Zaremba, Ilya Sutskever, Joan Bruna, Dumitru Erhan, Ian Goodfellow, and Rob Fergus. Intriguing properties of neural networks. *arXiv preprint arXiv:1312.6199*, 2013.
- [56] Hong Hui Tan and King Hann Lim. Two-phase switching optimization strategy in deep neural networks. *IEEE Transactions on Neural Networks and Learning Systems*, 33(1):330–339, 2022. doi: 10.1109/TNNLS.2020.3027750.
- [57] Vladimir Vapnik, Esther Levin, and Yann Le Cun. Measuring the vc-dimension of a learning machine. *Neural computation*, 6(5):851–876, 1994.
- [58] Ashish Vaswani, Noam Shazeer, Niki Parmar, Jakob Uszkoreit, Llion Jones, Aidan N Gomez, Lukasz Kaiser, and Illia Polosukhin. Attention is all you need. In *Advances in neural information processing systems*, pages 5998–6008, 2017.
- [59] Hao Wang, Naiyan Wang, and Dit-Yan Yeung. Collaborative deep learning for recommender systems. In *Proceedings of the 21th ACM SIGKDD international conference on knowledge discovery and data mining*, pages 1235–1244, 2015.
- [60] Han Xiao, Kashif Rasul, and Roland Vollgraf. Fashion-mnist: a novel image dataset for benchmarking machine learning algorithms, 2017.
- [61] Zhi-Qin John Xu, Yaoyu Zhang, Tao Luo, Yanyang Xiao, and Zheng Ma. Frequency principle: Fourier analysis sheds light on deep neural networks. *arXiv preprint arXiv:1901.06523*, 2019.
- [62] Sergey Zagoruyko and Nikos Komodakis. Wide residual networks. In *BMVC*, 2016.
- [63] Chiyuan Zhang, Samy Bengio, Moritz Hardt, Benjamin Recht, and Oriol Vinyals. Understanding deep learning (still) requires rethinking generalization. *Communications of the ACM*, 64(3): 107–115, 2021.
- [64] Hongyang Zhang, Yaodong Yu, Jiantao Jiao, Eric Xing, Laurent El Ghaoui, and Michael Jordan. Theoretically principled trade-off between robustness and accuracy. In *International Conference on Machine Learning*, pages 7472–7482. PMLR, 2019.
- [65] Jingfeng Zhang, Jianing Zhu, Gang Niu, Bo Han, Masashi Sugiyama, and Mohan Kankanhalli. Geometry-aware instance-reweighted adversarial training. *arXiv preprint arXiv:2010.01736*, 2020.
- [66] Shengyu Zhao, Zhijian Liu, Ji Lin, Jun-Yan Zhu, and Song Han. Differentiable augmentation for data-efficient gan training. *arXiv preprint arXiv:2006.10738*, 2020.
- [67] Yi Zhou and Yingbin Liang. Critical points of neural networks: Analytical forms and landscape properties. In *International Conference on Learning Representations*, 2018.